# Numerical Analysis of Coaxial Double Gate
## Schottky Barrier Carbon Nanotube Field Effect Transistors

M. Pourfath, E. Ungersboeck, A. Gehring, W.J. Park[1], B.H. Cheong[2],
H. Kosina, and S. Selberherr
Institute for Microelectronics, TU Vienna, Gußhausstraße 27–29, A-1040 Wien, Austria
[1] Materials and Devices Lab, [2] Computational Science and Engineering Lab,
Samsung Advanced Institute of Technology, Suwon 440-600, Korea
email: pourfath@iue.tuwien.ac.at

Carbon nanotubes (CNTs) have emerged as promising candidates for nanoscale field effect transistors. The contact between metal and CNT can be of Ohmic [1] or Schottky type [2]. Schottky contact CNTFETs operate by modulating the transmission coefficient of the Schottky barriers at the contact between the metal and the CNT [2, 3], but the ambipolar behavior of Schottky barrier CNTFETs limits the performance of these devices [4, 5]. We show that by using a double gate structure the ambipolar behavior of these devices can be suppressed. For simplicity we considered a coaxial geometry where the gate covers all around the CNT.

Assuming ballistic transport, we used a Schrödinger-Poisson solver for the analysis of Schottky barrier CNTFETs [6].

$$-\frac{\hbar^2}{2\mathrm{m}^*}\frac{\partial^2\Psi_\mathrm{s}}{\partial x^2} + (\mathrm{U} - \mathcal{E})\Psi_\mathrm{s} = 0 \qquad (1) \qquad \nabla^2\epsilon\phi = -\frac{\mathrm{q}(p-n)\delta(\rho-\rho_\mathrm{cnt})}{2\pi\rho} \qquad (2)$$

$$n_\mathrm{s} = \frac{4}{2\pi}\int f_\mathrm{s}|\Psi_\mathrm{s}|^2\mathrm{d}k_\mathrm{s} = \int \frac{\sqrt{2\mathrm{m}^*}}{\pi\hbar\sqrt{\mathcal{E}_\mathrm{s}}}f_\mathrm{s}|\Psi_\mathrm{s}|^2\mathrm{d}\mathcal{E}_\mathrm{s} \quad (3) \qquad I_\mathrm{d} = \frac{4\mathrm{q}}{\mathrm{h}}\int[f_\mathrm{s}(\mathcal{E}) - f_\mathrm{d}(\mathcal{E})]TC(\mathcal{E})\mathrm{d}\mathcal{E} \quad (4)$$

In (1) the effective mass was assumed to be $\mathrm{m}^* = 0.06\mathrm{m}_0$ [3]. In (2) $n = n_\mathrm{s} + n_\mathrm{d}$ and $p = p_\mathrm{s} + p_\mathrm{d}$ represent the contribution of the source and drain to the electron and hole concentrations calculated as (3), where $\delta$ is the Dirac delta function in cylindrical coordinate. Carriers were considered as charge sheets and because of cylindrical symmetry they were distributed uniformly over the surface of the CNT. The drain current is calculated within the Landauer-Büttiker formula as in (4) where $f_\mathrm{s,d}$ are equilibrium Fermi functions at the source and drain contacts and $TC(\mathcal{E})$ is the transmission coefficient through the device. The factor 4 in (3) and (4) stems from the twofold band and twofold spin degeneracy [2]. In this work we focus on ambipolar devices, where the metal Fermi level is located in the middle of the CNT band gap at each contact. All our calculations assume a CNT with $0.6$ eV band gap, corresponding to a diameter of $1.4$ nm [3]. First we consider a coaxial single gate CNTFET as in Fig. 1. Fig. 3 and Fig. 5 show the ambipolar behavior of this structure, in agreement with [4, 5]. To understand this behavior the band edge profile is shown in Fig. 4. Applying positive voltages higher than the gate voltage to the drain of n-type devices suppresses the Schottky barrier near the drain and consequently increases hole injection at the drain. In the off regime this results in a high off-current, and in the on regime the drain current increases with respect to the drain voltage instead of saturation. To avoid this phenomenon a coaxial double gate structure as in Fig. 2 can be used. If the drain voltage is applied to the second gate, at any drain voltage the band edge profile near the drain would be flat, see Fig. 4. In consequence the tunneling current of holes at the drain is suppressed, and there is just some thermionic emission current of holes which is nearly independent of the drain voltage, see Fig. 3. While electron injection at the source contact can be controlled via the first gate, the second gate suppresses parasitic hole current at the drain.

[1] A. Javey et al., Lett. to Nature **424**, 654 (2003).

[2] S. Heinze et al., Phys. Rev. Lett. **89**, 6801 (2002).

[3] J. Appenzeller et al., Phys. Rev. Lett. **92**, 8301 (2004).

[4] R. Martel et al., Phys. Rev. Lett. **87**, 6805 (2001).

[5] J. Guo et al., IEEE Trans.ED **51**, 172 (2004).

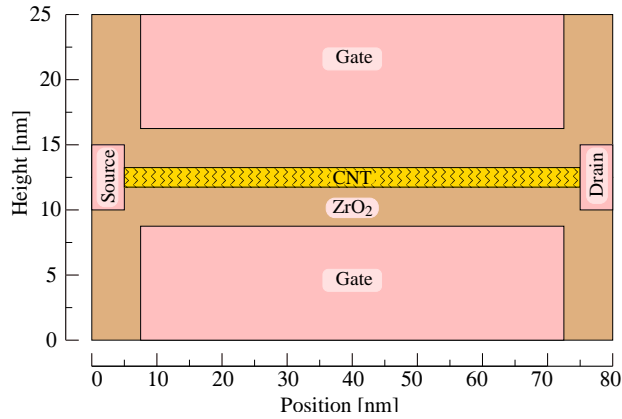[6] D. John et al., in *Proc. NSTI Nanotech* (2004).

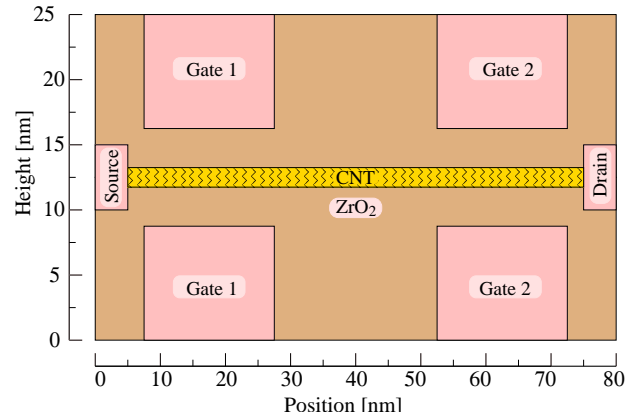**Figure 1:** 2D Sketch of the coaxial single gate (SG) structure.



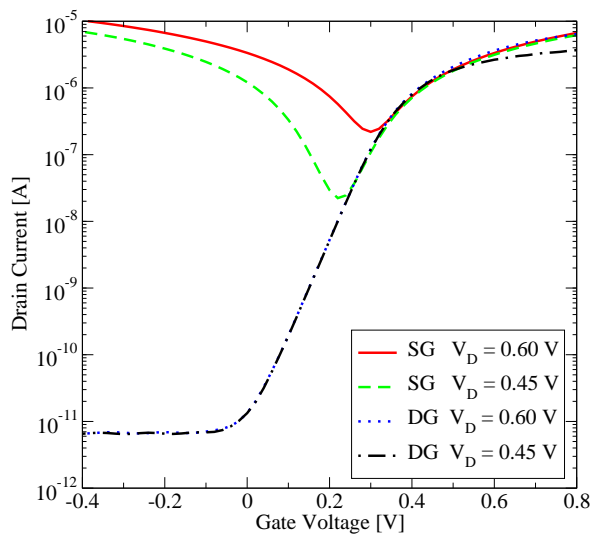**Figure 2:** 2D Sketch of the coaxial double gate (DG) structure.



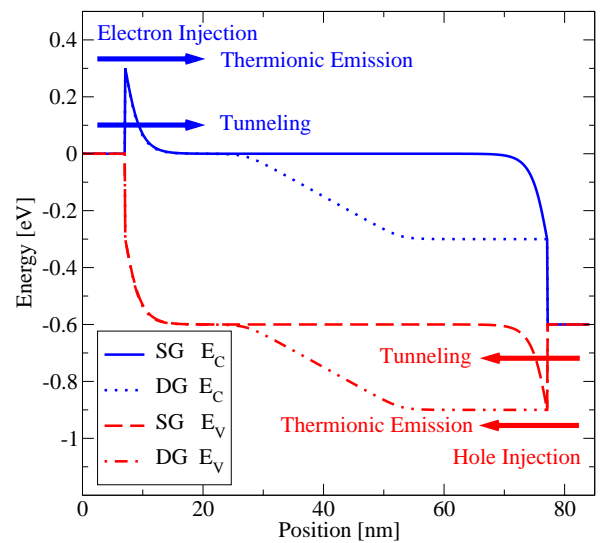**Figure 3:** I-V characteristics of the coaxial SG and DG structures.



**Figure 4:** Band edge profile of the coaxial SG and DG structures.
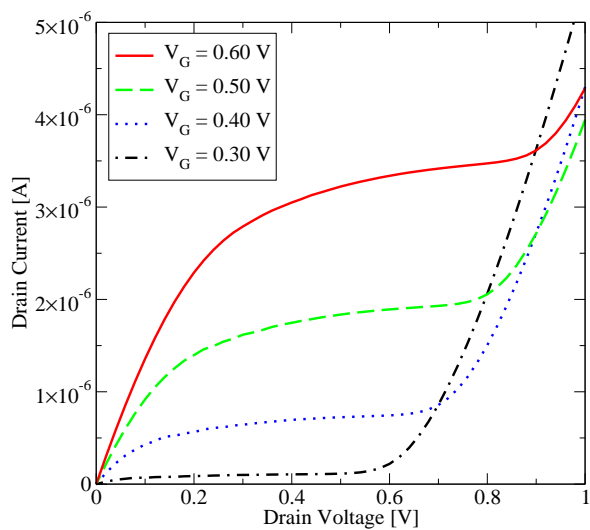


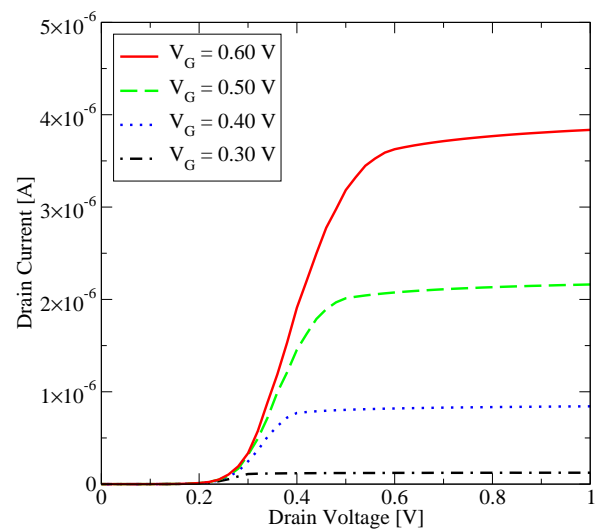**Figure 5:** I-V characteristics of the coaxial SG structure.



**Figure 6:** I-V characteristics of the coaxial DG structure.

A full journal publication of this work will be published in the Journal of Computational Electronics